Pr at Gd or Ba site in $GdBa_2Cu_3O_7$: Appearance of superconductivity

M. R. Mohammadizadeh and M. Akhavan*

Magnet Research Laboratory (MRL), Department of Physics, Sharif University of Technology, P.O. Box 11365-9161, Tehran, Iran

(Received 17 December 2002; revised manuscript received 22 April 2003; published 18 September 2003)

$Gd(Ba_{2-x}Pr_x)Cu_3O_{7+\delta}$ single phase polycrystalline samples with $0.0 \leqslant x \leqslant 1.0$ were investigated for their structural and electronic properties. Due to the solubility limit, the 123 structure forms in the $0.0 \leqslant x \leqslant 0.50$ range; for $x \geqslant 0.6$, a decomposition of the perovskite-type phases occurs. For $x = 0.2$, there is an orthorhombic-tetragonal phase transition, concurrent with a metal-insulator transition, which is evident in the normal state resistivity. For $x_c = 0.35$, the superconductor-insulator transition occurs. An unusual hump has been observed on the resistivity vs temperature curve of the samples for particular values of Pr doping. Based on the Rietveld refinement of the x-ray diffraction patterns, and bond valence sum calculations, we have found that the Ba atom substitution at the rare earth site could lead to superconductivity in some parts of the grains at $T_m \sim 80-90$ K, which appears as a hump on the $\rho(T)$ curve. Our result is in line with the previously proposed possibility of the existence of superconductivity in Pr-123 due to the Ba atom substituted at the Pr site. We have also concluded that with increasing Pr doping, O(4) atoms migrate from their sites, and the O(5) occupation increases. So, perovskite substructures with Pr at the rare earth or Ba site, become identical. Hence, Pr at the Ba or rare earth site suppresses the superconductivity by the same mechanism(s).

DOI: 10.1103/PhysRevB.68.104516 PACS number(s): 74.25.Fy, 74.62.Dh, 74.72.Bk

INTRODUCTION

The $PrBa_2Cu_3O_{7-\delta}$(Pr-123) compound in the orthorhombic phase, in contrast to other R-123 (R=Y or rare earth) compounds, is an insulator.[1,2] Different theories have been proposed for explaining the insulating Pr-123, i.e., hole filling,[3] pair breaking,[4] and hybridization.[5] Also, some groups have reported the observation of superconductivity in the powder, single crystal, polycrystalline, and thin films of this compound.[6] Therefore, the phenomenon of the Pr-123 system has become more complicated: The question is under what conditions, if ever, the Pr-123 compound could become a superconductor. Recently, the role of Pr in high temperature superconductors (HTSCs) has been reviewed by Akhavan.[7]

The substitution of Pr at the Ba site (Pr_{Ba}) (mis-substitution effect) has also been proposed.[8] This proposal seems relevant due to the nearly equivalent positions of R and Ba sites in the center of the imperfect R-123 perovskite structure, and the fact that superconductivity is suppressed in $R(Ba_{2-x}R'_x)Cu_3O_{7+\delta}$ compounds (R'=rare earth, not necessarily the same atom as in R).[9] To account for the larger c lattice parameter in the superconducting Pr-123 samples, Zou *et al.*[10] have suggested the mis-substitution of larger Ba atoms on the Pr site. In addition, Narozhnyi and Drechsler[11] inferred from the inconsistency of the value of μ_{eff} of Pr, reported by Zou *et al.*[10]—which has also been confirmed by Zou and Nishihara[12]—that Pr occupies only about half of the R sites. The other half of the R sites is probably occupied by the nonmagnetic Ba atoms. Further, based on the phonon Raman scattering measurements in $Pr_{1+x}Ba_{2-x}Cu_3O_{7-\delta}$ samples,[13] it has been concluded that Pr substitution on Ba sites occurs even for a very small value of Pr doping x. Moreover, Muroi *et al.*[14] have claimed that the appearance of superconductivity in Pr-123 is extrinsic in origin; both Pr-site Ba ions and Ba-site Pr ions change crystal structure, and modify the energy levels at the Cu and Pr sites in such a way as to be unfavorable for Pr-O hybridization, and favorable for holes in the Cu^{3+} oxidation state.

To evaluate the validity of the mis-substitution effect further, the $Eu(Ba_{2-x}Pr_x)Cu_3O_{7-\delta}$ compound has been studied,[15] and it was found that the $Eu(Ba_{1.3}Pr_{0.7})Cu_3O_{7-\delta}$ compound is still a superconductor with $T_c^{\text{onset}} = 7.1$ K. The authors have concluded that in these compounds, Pr at the Ba site does not have such a strong effect on superconductivity as assumed by Blackstead and Dow in terms of mis-substitution.[16] Another claim against mis-substitution is that the site selectivity and local structure sensitivity afforded by the extended x-ray absorption fine structure (EXAFS) techniques allowed Harris *et al.*[17] to conclude that Pr does not substitute for Ba in the Pr-123 compound in amounts greater than 1%. This result precludes the possibility of Ba-site Pr as a source of superconductivity suppression in Pr-123.

Therefore, the mis-substitution of Pr and Ba in their relevant sites could take place in the 123 structure, while the extent of its effects is yet controversial. An appropriate means to understand the effects of Pr at the Ba site is to study the $R(Ba_{2-x}Pr_x)Cu_3O_{7+\delta}$, and compare it with the $(R_{1-x}Pr_x)Ba_2Cu_3O_{7-\delta}$ compound. In this paper, we will present structural data on the $Gd(Ba_{2-x}Pr_x)Cu_3O_{7+\delta}$ compound. The comparison of the electronic and structural properties of this system with the $(Gd_{1-x}Pr_x)Ba_2Cu_3O_{7-\delta}$ compound[18] will clarify the effects of Pr substitution at the rare earth or Ba site, as well as the possibility of superconductivity in a Pr-123 system. In the resistivity vs temperature curve of $Gd(Ba_{2-x}Pr_x)Cu_3O_{7+\delta}$ samples we have observed a hump above T_c for some particular Pr doping values. We will also explain several possible scenarios to account for the resistance anomaly. Our final conclusion is important for resolving the ρ-T anomaly and the possibility of superconductivity in the Pr-123 system.

EXPERIMENTAL AND COMPUTATIONAL DETAILS

$Gd(Ba_{2-x}Pr_x)Cu_3O_{7+\delta}$ single phase samples with x = 0.00, 0.05, 0.10, 0.15, 0.20, 0.25, 0.30, 0.35, 0.40, 0.50,

0.60, 0.80, and 1.00 were synthesized by the standard solid state reaction technique. In accordance with the procedures followed in our previous report,[19] appropriate amounts of Gd_2O_3, Pr_6O_{11}, $BaCO_3$, and CuO powders with 99.9% purity were mixed, ground, and calcined at 840 °C for 24 h in an air atmosphere. Calcination was repeated twice with intermediate grinding. Then, powders were reground, pressed into pellets, and synthesized at 930 °C for 24 h in an oxygen atmosphere. The samples were cooled to 550 °C and retained under oxygen flow for 16 h. Finally, they were furnace cooled to room temperature. The oxygen content of samples has been determined by the iodometric titration technique with ± 0.03 accuracy.

The scanning electron microscopy (SEM) measurements have been done to determine the grain size and homogeneity of the samples by the JEOL-JXA-840 instrument. The x-ray diffraction (XRD) measurements have been done by a Philips PW-3710 powder diffractometer with Cu K_α radiation and $\lambda = 1.5406$ Å at room temperature with a 0.02° step width and a 0.5 second step time. The XRD results have been analyzed with the DBW3.2S-PC-9207 package based on the Rietveld method.[20] In the refinements of up to 27 parameters, including the scale factor, cell parameters (*a*, *b*, and *c*), atomic coordinates, isotropic displacements (*B*), site occupation factors (*N*), and profile shape parameters were allowed to vary. The *B* of the oxygen atoms was fixed to 1.0 Å.[21] The background was refined and a Lorentzian profile function was used for all samples. The refinements were based on diffraction data in the range $5° \leqslant 2\theta \leqslant 120°$ containing 37 reflections from the orthorhombic phase and 32 reflections from the tetragonal phase. The accuracy of the lattice parameters for *a* and *b* is at most 0.0005 Å and for *c* is 0.002 Å. The accuracy of N, B, and Z in the Rietveld refinements are at most 0.01, 0.4, and 0.003 Å, respectively.

An ac four-probe method with $f = 33$ Hz was used for the conductivity measurements of the samples within the temperature range of 10–300 K. The size of the samples was about $8 \times 3 \times 2$ mm^3. The electrical contacts were attached to the long side of the samples by silver paste. A Lake Shore-330 temperature controller with two Pt-100 resistors was used for controlling and measuring the temperature to within ± 10 mK. Different currents from 10 to 100 mA were applied in resistivity measurements. For the magnetoresistivity measurements a magnetic field of maximum value 20 kOe was used. The ac susceptibility measurements have been undertaken using a Lake Shore-7000 ac susceptometer. The ac susceptibility was measured in a 333-Hz ac magnetic field, and for any measurement, the sample was cooled down to liquid nitrogen temperature in zero field and then warmed up at a constant rate of 0.2 K/min.

The bond valence sum (BVS) around any atom by Gauss' law is equal to the formal ionic charge of that ion; experimental studies have shown that it correlates closely with the bond length. Thus, the bond lengths can be used to determine bond valences. The BVS for atom *i* is

$$V_i = \Sigma s_j = \Sigma \exp[(R_0 - R_{ij})/B_0],$$

where s_j is the valence of one bond, and the sum is over all neighbors *j*; the constant $B_0 = 0.37$ was empirically determined.[22] R_0 represents the length of a bond of unit valence, and R_{ij} is the distance between atoms *i* and *j*. The used R_0 for different atoms and their references are presented in Table I. The copper bond valence sums were calculated using the formulas suggested by Tallon,[24] with $V_{Cu} = (3V_2 - 2V_3)/(V_2 + 1 - V_3)$ if $V_2 > 2$, and $V_{Cu} = (V_2 - 2V_1)/(V_2 - 1 - V_1)$ if $V_2 < 2$, where V_1, V_2, and V_3 are the BVS values for Cu^{1+}, Cu^{2+}, and Cu^{3+}, respectively. The BVS for Pr was calculated in an analogous way by $V_{Pr} = (4V_3 - 3V_4)/(V_3 + 1 - V_4)$, where V_3 and V_4 are the BVS values for Pr^{3+} and Pr^{4+}, respectively. The BVS for Pr was obtained to be used in calculating the BVS for oxygen. It should be noted that the BVS for Pr has been calculated using the average distances between the rare earth ion and the surrounding oxygen, and therefore, it should not be given particular attention. However, an error in the Pr valency due to its low doping level has only a small influence on the oxygen valences. The BVS for oxygen was calculated by taking into account the amount of Cu^{1+}, Cu^{2+}, Cu^{3+}, Pr^{+3}, and Pr^{+4}. If the bond lengths are determined to within a 10^{-4} Å accuracy, the valences would be exact to a 10^{-3} electronic charge.

TABLE I. The used R_0 for different atoms with their references.

Cation	R_0(Å)	References
Cu^{+1}	1.600	23, 24
Cu^{+2}	1.679	23, 24
Cu^{+3}	1.730	23, 24
Ba^{+2}	2.285	22
Gd^{+3}	2.077	22
Pr^{3+}	2.138	22
Pr^{4+}	2.154	25

RESULTS AND DISCUSSION

The SEM topographs of the samples show a homogeneous granular structure with micrometer grain size. Figures 1 and 2 show typical XRD patterns for $Gd(Ba_{1.95}Pr_{0.05})Cu_3O_{7.03}$ and $Gd(Ba_{1.80}Pr_{0.20})Cu_3O_{7.01}$ samples, respectively. It shows that a single phase of a 123 structure has been formed, and that there is no considerable impurity phase. The (200) and (020) peaks near $2\theta = 47°$ in the $x = 0.05$ sample are characteristic of the existence of an orthorhombic phase as in the $YBa_2Cu_3O_{7-\delta}$ system.[26] So, for $0.0 \leqslant x \leqslant 0.15$, an orthorhombic structure with *Pmmm* symmetry, and for $0.2 \leqslant x \leqslant 0.5$, a tetragonal structure with *P*4/*mmm* symmetry, have been used in the refinements. The total site occupation factors for O(1) and O(5) atoms (chain and antichain oxygens, respectively) were set to the iodometric measurement results as presented in Table II. In $(R_{1-x}Pr_x)Ba_2Cu_3O_{7-\delta}$ compounds just before the main peak at $2\theta \cong 31°$, the impurity peaks of the $BaCuO_2$ phase are unavoidable.[27] The existence of this impurity phase has been attributed to the *R* occupation of the Ba site, which causes the extra Ba atoms to form a new phase (impurity phase). However, in the $Gd(Ba_{2-x}Pr_x)Cu_3O_{7+\delta}$ compound,

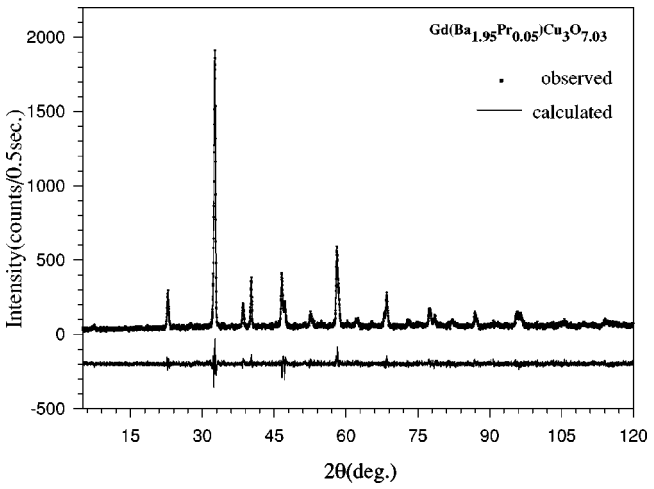

FIG. 1. The observed XRD pattern, the Rietveld refinement calculation, and their differences (at the bottom) for the $x=0.05$ sample.

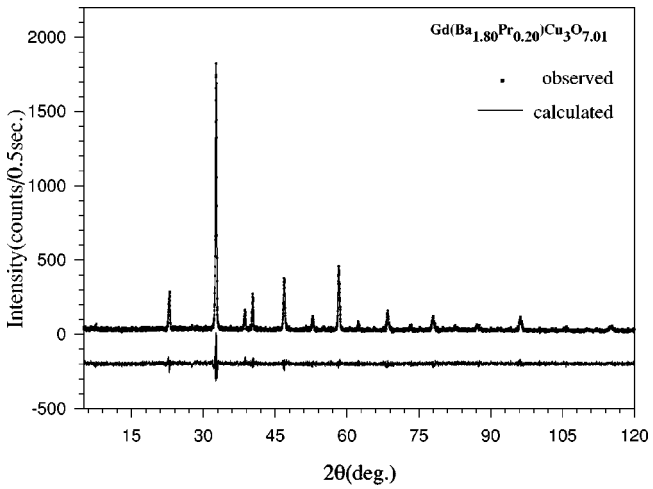

FIG. 2. The observed XRD pattern, the Rietveld refinement calculation, and their differences (at the bottom) for the $x=0.20$ sample.

a noticeable impurity phase including Ba has not been observed. This shows that in this compound Ba atoms participate fully in the structure. If Pr atoms, instead of occupying the Ba sites, had preferred the *R* sites, there should have been some extra Gd atoms left to participate in an impurity phase; the absence of any impurity phase formed by Gd is evidence that the 123 structure of the $Gd(Ba_{2-x}Pr_x)Cu_3O_{7+\delta}$ compound has been formed.

For $x \geqslant 0.6$, the XRD patterns indicate that the 123 structure has not been formed, and their resistivities are a few orders of magnitude larger than for the $x<0.6$ samples. Due to the different charges and atomic sizes of Ba^{2+} and R^{3+} ions, the 123 structure can only exist for a certain region of R^{3+} substitution for Ba^{2+}. The solubility of *R* ions at the Ba site depends on the size of rare earth ion. The larger the rare earth ion, the larger its solubility limit; La has the highest solubility at the Ba site with $x \approx 0.7$, and Y has the lowest solubility, which is a point compound in the phase diagram.[28] The solubility limit of $R(Ba_{2-x}R_x)Cu_3O_{7+\delta}$ with $R=$Sm and Eu is $x \leqslant 0.5$,[29] and for $R=$Nd is $x \leqslant 0.6$ (Ref. 28); for $x>0.5$, decomposition of the perovskite-type phase occurs and the impurity phase of K_2NiF_4-type shows up in the XRD patterns of Sm and Eu at $x=0.6$.[29] This may indicate that the block stones of the 123 structure are incomplete perovskites. Under appropriate conditions, the perovskites mach to each other and a 123 structure forms; however, in the others, just the perovskite-type substructures are preferable.

Variation of lattice parameters with the amount of Pr doping (x) are shown in Fig. 3. The lattice parameter *a* increases and *b* decreases till for $x=0.2$ the orthorhombic-tetragonal (*O*-*T*) phase transition occurs. This transition is due to the O(5) (0.5,0.0,0.0) occupation, which is due to the appearance of Pr^{3+} at the Ba^{2+} site, and requiring a more negative charge. At $x=0.2$, the coexistence of O(1) chain and O(5) antichain oxygen make the *a* and *b* directions equivalent, and the tetragonal phase forms. This *O*-*T* transition has also been reported in other $R(Ba_{2-x}R'_x)Cu_3O_{7+\delta}$ systems:[9,30–33] In $Pr(Ba_{2-x}La_x)Cu_3O_{7+\delta}$ at $x=0.45$,[30] in $Pr(Ba_{2-x}Pr_x)Cu_3O_{7+\delta}$ at $x=0.4$,[34] and in $Sm(Ba_{2-x}Pr_x)Cu_3O_{7+\delta}$ at $x=0.35$.[31] Neutron data of $Nd(Ba_{2-x}Pr_x)Cu_3O_{7+\delta}$ also indicated[9] that Pr, when it occupied the Ba site, resulted in the *O*-*T* transition, and further behaved like all other trivalent rare earth ions. There is also a competition between two opposite requirements. On the one hand, oxygen is needed to counterbalance the heterovalent substitution and, on the other hand, occupancy of the O(5) site should stay as low as possible to achieve a coordination number close to 8 for a Pr atom at the Ba site. Regardless of the structural change, the *c* lattice parameter and unit cell volume (v) decrease with increasing *x*, which is due to replacing the larger Ba^{2+} ion with the smaller Pr^{3+} ion. In the $(Gd_{1-x}Pr_x)Ba_2Cu_3O_{7-\delta}$ system, however, there is no *O*-*T* transition with increasing *x*; all of *a*, *b*, *c*, and *v* increase in replacing the larger Pr^{3+} ion with the smaller Gd^{3+} ion. This also indirectly shows that, in our samples, Pr has been substituted at the Ba site, and not at the Gd site.

The measured mass densities of the samples are presented in Table II. The mass density decreases by replacing the larger and lighter Ba atom with the smaller and heavier Pr atom in the Gd-123 structure. Under the same preparation

TABLE II. Oxygen content of $Gd(Ba_{2-x}Pr_x)Cu_3O_{7+\delta}$ samples obtained by iodometric titration and the measured mass density for different amounts of Pr doping (x).

x	0.00	0.05	0.10	0.15	0.20	0.25	0.30	0.35	0.40	0.5
$7+\delta$	6.99	7.03	7.03	7.09	7.01	7.06	7.06	6.97	6.99	6.96
Density(gr/cm^3)	5.47	4.32	5.43	4.26	4.65	4.62	4.61	4.89	4.48	4.29

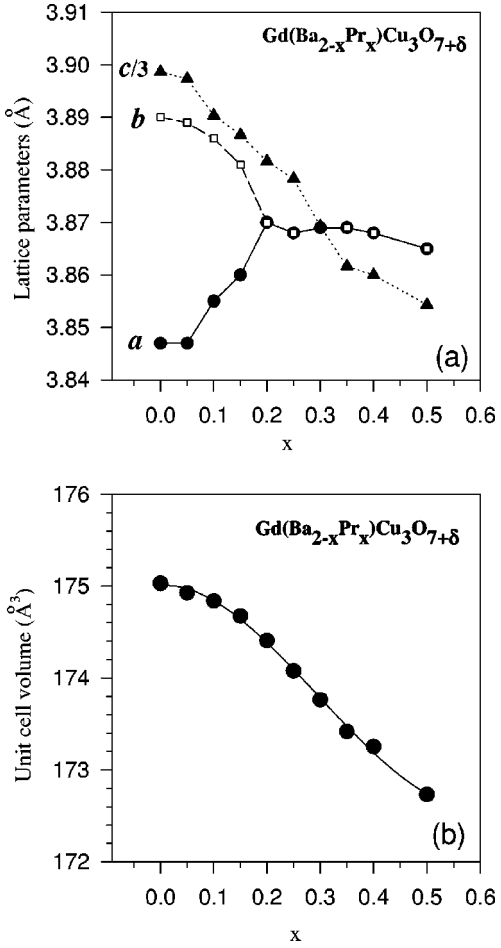

FIG. 3. (a) Variation of lattice parameters. (b) Unit cell volume vs amounts of Pr doping (x). The lines are guides to the eye.

conditions, the mass density should increase with increasing x, while it decreases. This shows that Pr substitution increases the porosity of the samples, which is due to the increase of the decomposition temperature with increasing of Pr concentration.

Figure 4 shows a typical temperature dependence of the real (χ') and imaginary (χ'') parts of the ac susceptibility for $x=0.00$ sample. The Meissner effect and bulk superconductivity are evident from the figure. The onset temperature of the intrinsic superconducting transition is about 90 K. The resistivity of the samples have been measured at $I=10$ mA and presented in Fig. 5. The details of the normal state conduction of this system have been presented in Ref. 35. With the increase of x, the superconducting transition temperature decreases and the width of the transition temperature (ΔT_c) as well as the normal state resistivity increase, similar to the $(Gd_{1-x}Pr_x)Ba_2Cu_3O_{7-\delta}$ system.[36] With the increase of the number of insulating parts in the grain (i.e., Pr substituted unit cells), the homogeneity of grains decreases, which leads to a larger ΔT_c.

The normal state resistivity for $x<0.2$ samples is metallic ($d\rho/dT>0$), and for $x>0.2$ is semiconductinglike ($d\rho/dT<0$). So, the critical doping for the metal-insulator transition (MIT) is $x_c^{\mathrm{MIT}}=0.2$. In the metallic samples, the linear part of $\rho(T)$ from room temperature down to T_c, decreases with

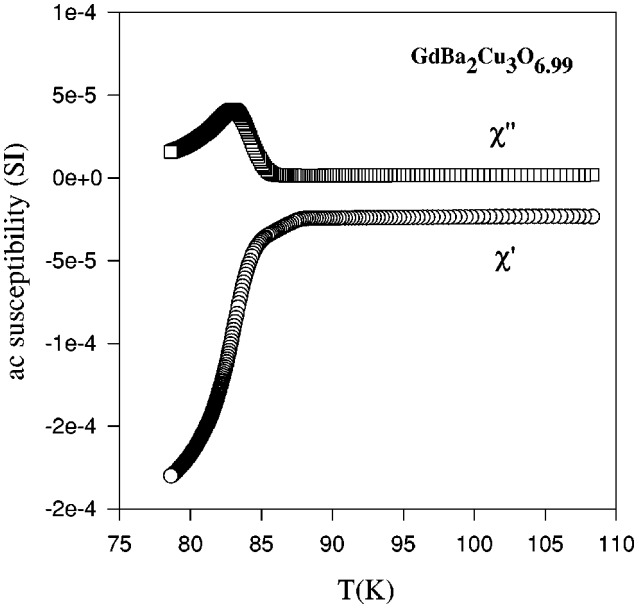

FIG. 4. The real (χ') and imaginary (χ'') parts of the ac susceptibility for the $GdBa_2Cu_3O_{6.99}$ sample.

increasing Pr doping. This corresponds to the doping dependence of the pseudogap, which is beyond the scope of this paper. In the samples with $x\leqslant 0.35$, the superconducting transition occurs, while for $x\geqslant 0.4$ there is no transition down to 10 K. So, the critical doping for superconductor-insulator transition (SIT) is $x_c^{\mathrm{SIT}}=0.35$. It is important to distinguish the difference between the critical x for the SIT and MIT. The value of x_c^{SIT} in this compound is less than the one for $(Gd_{1-x}Pr_x)Ba_2Cu_3O_{7-\delta}$ compound, i.e. 0.45.[36] This means that the superconducting suppression by Pr positioned at the Ba site is more effective than Pr at the R site. For the

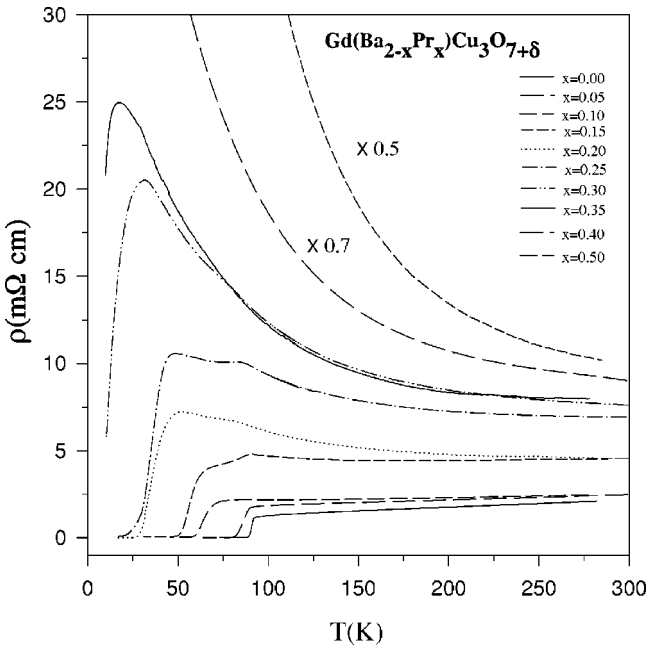

FIG. 5. Resistivity curve for $Gd(Ba_{2-x}Pr_x)Cu_3O_{7+\delta}$ samples in the range 10 K$<T<$300 K for $0.0\leqslant x\leqslant 0.5$.

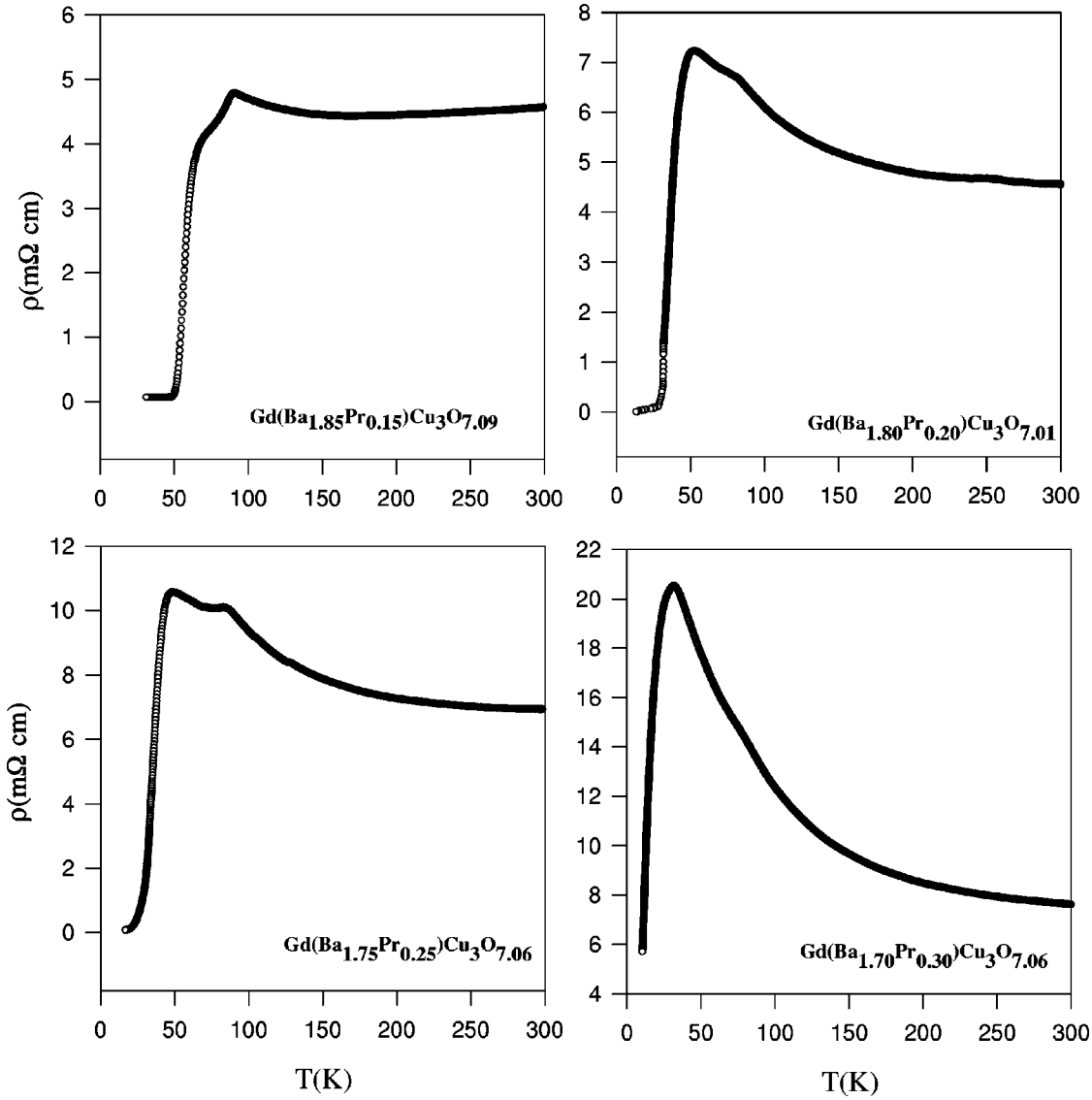

FIG. 6. The hump on the resistivity curve of $Gd(Ba_{2-x}Pr_x)Cu_3O_{7+\delta}$ for the $x=0.15$, 0.20, 0.25, and 0.30 samples at $T\sim 80-90$ K.

Pr at the R site, we have an isovalent substitution of R^{3+} by Pr^{3+}, while in the Pr^{3+} at the Ba^{2+} site, an effect on carrier density is expected due to different valency of Pr^{3+} and Ba^{2+}. This is also supported by Table II, proving that valence variation is not balanced by the change of oxygen content. Another plausible explanation for this is that the Ba site is located between the CuO_2 superconducting plane and Cu-O charge reservoir chains,[37] which both have proved to be essential for superconductivity of 123 systems. Hence, the existence of Pr atoms between these two correlated parts would be more destructive than when Pr is positioned at the R site, which is between the two independent CuO_2 planes.

The resistivity of the $x=0.15$, 0.20, 0.25, and 0.30 samples are presented in Fig. 6. There is a hump present on the curves above T_c at $T_m\sim 80-90$ K. This hump is different from the S-shaped curvature in the resistivity vs temperature curve, which happens and develops with Pr doping.[38] The S-shaped curvature is characteristic of either oxygen depletion[39] or cation substitutions for chain Cu atoms.[40] Figure 7 shows the variation of T_c and hump temperature (T_m) vs x for all the samples showing the hump. The hump on the resistivity curve is present only for some particular values of x. So, this cannot be due to some characteristic structural modification, but this special feature occurs only for some particular dopings. It should be emphasized that these humps are reproducible through different measurements, and are not due to any measurement errors. In addition, there is no impurity phase evident in the XRD spectrums in the $0.10\leqslant x \leqslant 0.30$ range, meaning that the impurity phase cannot be the origin of these humps (Fig. 2). Similar peaks on the resistivity curves of $Y_{1-x}Pr_xBa_2Cu_3O_{7-\delta}$,[41] and $EuBa_2Cu_3O_{7-\delta}$ (Ref. 42) compounds, have been observed just above their superconducting transition temperatures. Of course, no explanations have been presented by the authors for the anomalous humps. A point to note is that the peak positions are at $T\sim 80-90$ K, the same as the data for our samples. This observation would be useful in guiding our following speculations.

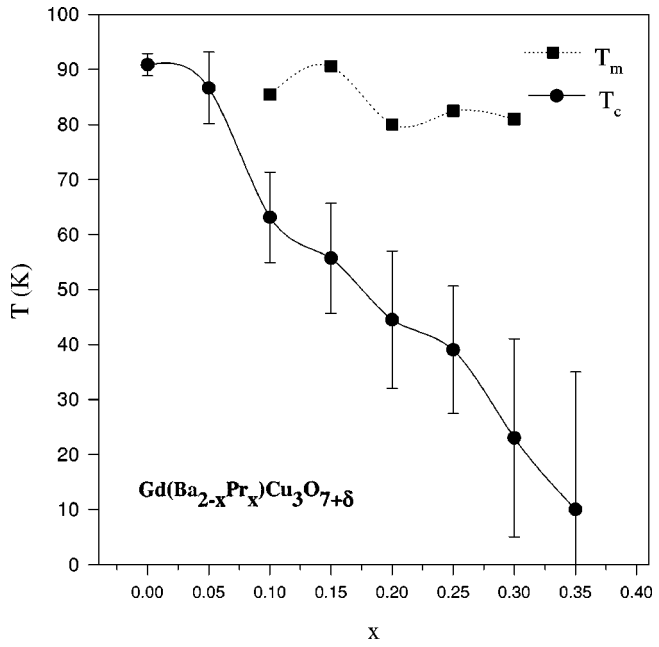

FIG. 7. Variation of the superconductivity transition temperature (T_c) and the temperature at which the resistivity hump occurs (T_m) vs different amounts of Pr doping (x). The vertical lines are the width of superconducting transition (ΔT_c). The lines through the points are a guide to the eye.

The $x=0.0$, 0.1, and 0.2 samples were prepared in one batch, the $x=0.05$, 0.15, and 0.25 in another batch, and the $x=0.30$, 0.40, and 0.50 in a third batch, with exactly the same fabrication procedures. As some of the samples in each batch show the hump on their ρ-T curves, it is evident that the difference in sample preparation procedures could not have caused these humps. The hump on ρ-T curve is not very broad as has been observed in the $PrBa_2Cu_4O_8$ (Pr-124) compound at about 160 K.[43] Although, the origin of this peak remains still unclear, but it has recently been discussed in terms of possible structural instability of the Pr-124 lattice at the given temperature.[44] However, our samples show superconductivity, which does not occur in the Pr-124 compound at least down to 2 K.[45] So, it seems that our case is different from the Pr-124 anomaly.

In the under-doped $La_{2-x}Sr_xCuO_4$ single crystals a small peak above T_c have been reported in the CuO_2 plane resistivity (ρ_{ab}). With the assumption of no ρ_c interference in ρ_{ab}, the peak was related to an electronic phase transition from a nematic stripe phase to a more ordered smectic one ("stripe glass").[46] In polycrystalline samples, the measured resistivity is an effective resistivity along the CuO_2 planes and the c direction. So, it makes it improbable to imply the relevancy of this argument for our samples. Authors have also mentioned that crystal inhomogeneities could be the origin of the anomaly. It should also be noted that the hump on the ρ-T curve does not depend on the cooling or heating sequences. It means that there is no hysterisis on the ρ-T curve by decreasing and subsequent increasing of the temperature.

In ac susceptibility measurements of our samples, which showed no humps either in the real part or in the imaginary part, no anomalous behavior was observed at T_m. On the other hand, in the post annealed $Pr_{2-x}Ce_xCuO_{4-\delta}$ samples, a sudden drop in the $\rho(T)$ starting around 20 K together with a peak in the imaginary part of the ac susceptibility have been supposed as evidences of the inhomogeneous samples.[47] The reason that our ac susceptibility measurements do not show anomalous peaks for our samples at T_m could be the closeness of T_m to the minimum possible ac susceptibility measuring temperature (liquid nitrogen). Hence, due to the limitations in our ac susceptibility measurements, we could not be sure about the presence of any inhomogeneity in our samples.

Table II shows the amount of oxygen content ($7+\delta$) in our samples with different Pr dopings (x). It is evident that the oxygen contents in the samples have the expected contents[34] with no deficiency. So, we can rule out the orthorhombic-tetragonal transition at the hump temperature due to oxygen deficiency. However, in the 123 structure, such a phase transition takes place at $T\sim 60$ K,[48] and not at $T\sim 80$ K, where we have seen the anomaly in the resistivity curve.

To evaluate the origin of the humps further, different currents from 10 to 100 mA and magnetic fields up to 20 kOe were employed on the samples. It was concluded that these factors made no changes on the humps. Since the current and magnetic field required for intergranular effects are less than or equal to the applied currents and magnetic fields on our samples,[49] it is concluded that the origin of the hump cannot be related to the intergranular regions. To clarify the case with further evidence, the temperature dependence of the resistivity for the $(Sr_{0.86}Pr_{0.14})CuO_2$ sample shows a two-step transition,[50] which is similar to our case. This effect is often observed in some electron doped superconducting compounds $L_{2-x}M_xCuO_{4-\delta}$ (L=Pr,Nd,Sm,Eu; M=Ce,Th).[51] This double-step transition at T_m has been related to the small volume fraction of the superconducting phase in the sample,[50] and it is explained in terms of the intragranular and intergranular superconducting transitions. The authors have claimed that at T_m some parts of the grains become superconducting. So, the resistivity decreases, but the intragranular supercurrent could not easily transmit from the Josephson junctions between the grains. Therefore, the resistivity does not decrease to zero till the Josephson coupling energy exceeds the thermal energy of the order of k_BT. Then, the superconducting transition occurs. This explanation seems justifiable for our samples if we could find evidences for some superconducting regions at T_m. This attempt is made in the following.

The typical observed XRD patterns, the calculated spectrum by the Rietveld method, and their differences for $x=0.05$ and 0.20 samples are presented in Figs. 1 and 2, respectively. When we used the fixed site occupation factors for atoms in the compound, the negative isotropic displacements (B) was found for some atoms; the $Z_{O(4)}$ was found to be $\sim$0.13, which should have been about 0.16; the $Z_{O(2)}$ was found to be less than $Z_{Cu(2)}$, which should have been more than $Z_{Cu(2)}$.[40] When the occupation factor of the atoms was

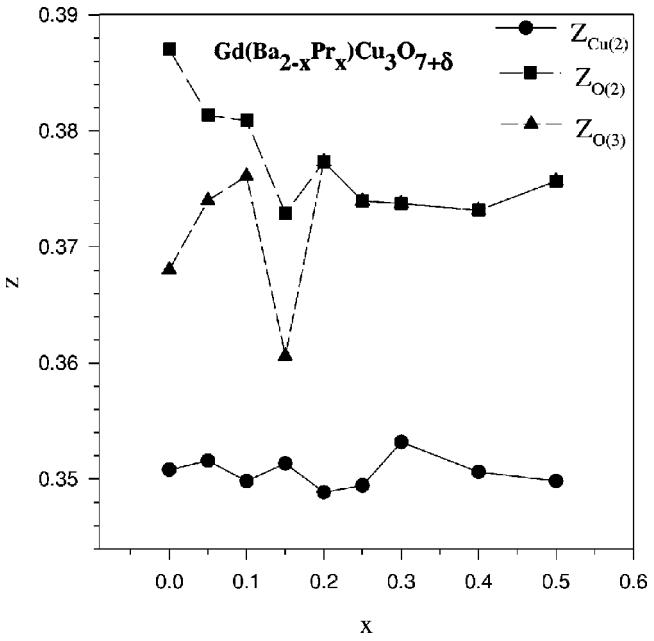

FIG. 8. Relative position of atoms in the CuO_2 plane in the c direction vs different amounts of Pr doping (x): For $x \geqslant 0.20$, O(2)=O(3) due to the orthorhombic-tetragonal phase transition. The lines through the points are a guide to the eye.

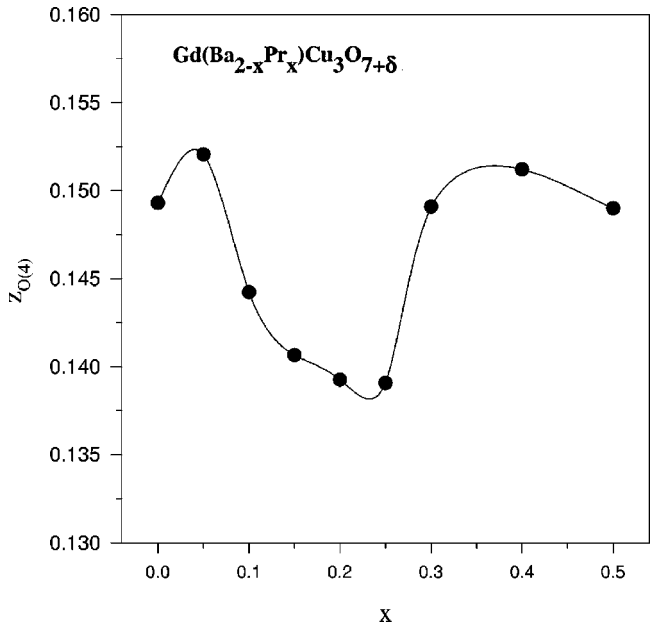

FIG. 9. Relative position of apical oxygen [O(4)] in the c direction ($Z_{O(4)}$) vs different amount of Pr doping (x). For $0.10 \leqslant x \leqslant 0.25$, the underestimation of $Z_{O(4)}$ is evident. The line through the points is a guide to the eye.

set as variables, the B of the atoms did not become negative, but some anomaly was still observed in the positions of the atoms. Figure 8 shows the positions of O(2), O(3), and Cu(2) atoms in the unit cell for different x. From the $Z_{Cu(2)}$-x curve it is evident that for $0.1 \leqslant x \leqslant 0.25$, the position of the Cu(2) atom is lower than the expected value from the curve; the $Z_{O(2)}$ and $Z_{O(3)}$ at $x=0.15$ are obviously out of the expected range (Fig. 8). The O(4) atomic position vs x shows the same anomaly in the range $0.1 \leqslant x \leqslant 0.25$, as presented in Fig. 9. The decrease in the values of $Z_{O(2)}$, $Z_{O(3)}$, and $Z_{Cu(2)}$ can be understood if a large atom, larger than the typical R atomic size, is substituted at the R site, which could push away the CuO_2 plane, i.e., an elongation of the distances between the CuO_2 planes. The larger atom, probably with a positive charge, but a smaller charge than Gd^{3+}, pushes away the $O(2)^{2-}$ and $O(3)^{2-}$ anions. This reduction in the value of the positions of O(2) and O(3) atoms could also prevent the O(4) atom from occupying its expected equilibrium position. The Ba atom is the most probable candidate to fit this scenario, as it has the larger ionic radius ($r_{Ba^{2+}} > r_{Pr^{3+}} > r_{Gd^{3+}}$), and smaller ionic charge (+2).

To test the above proposal, we have repeated the Rietveld refinement with the allowance of Ba atoms to relocate at the R site (Ba_R) for all values of x. The final results of the Rietveld refinement are presented in Table III. These include lattice parameters (a, b, and c), site occupation factor (N), isotropic displacement (B), relative position of atoms in c direction (Z), R factors of the Rietveld refinement [pattern R factor (R_p), weighted pattern R factor (R_{wp}), Bragg R factor (R_B), structure R factor (R_F)], and the goodness of fit parameter (S), which are presented for the following positions of atoms: Gd(0.5,0.5,0.5), Ba(0.5,0.5,Z_{Ba}), Pr(0.5,0.5,Z_{Pr} $=Z_{Ba}$), Cu(1)(0.0,0.0,0.0), Cu(2)(0.0,0.0,$Z_{Cu(2)}$), O(1)(0.0,0.5,0.0), O(2)(0.5,0.0,$Z_{O(2)}$), O(3)(0.0,0.5,$Z_{O(3)}$), O(4)(0.0,0.0,$Z_{O(4)}$), and O(5)(0.5,0.0,0.0). For $x \geqslant 0.2$ (tetragonal phase) $a=b$, $Z_{O(2)}=Z_{O(3)}$, and O(1)≡O(5). The goodness parameter of refinement S, is close to 1, which is in support of the reliable results.[19] The interesting result is that for the special values of $0.05 \leqslant x \leqslant 0.30$, the Ba atom occupies the R site (Fig. 10); the Ba_R mis-substitution has the highest value at $x=0.2$. This domain of x almost corresponds to the domain of x for which hump appears on the ρ-T curves (Table III). However, for $x=0.05$, the temperature at which the hump appears could be within the transition width, and for $x=0.3$, the amount of mis-substitution is negligible. It would be interesting to find a relation between the Ba_R and the ρ-T anomaly. The difference of Gd site occupation factor (N) from 1 may correspond to some vacancies in unit cells. These unit cells apparently have a 123 structure, since they do not contribute to any impurity peaks in the XRD patterns. Where, the Ba_R mis-substitution is considerable, $0.1 \leqslant x \leqslant 0.25$, the position of the apical oxygen in the c direction ($Z_{O(4)}$) is lower than for the other x values. This is due to the Ba_R, which pushes the CuO_2 plane down. This lowering of the value of O(2) and O(3) positions could also lower the position of O(4) atom from its expected equilibrium position.

In the Zou's superconducting Pr-123 samples,[10] one possibility for the larger c lattice parameter with respect to the typical 123 structures has been proposed to be the presence of Ba atoms at Pr site (Ba_R). Narozhnyi and co-workers,[11,52] based on the effective magnetic moment of the Pr atom, have concluded that in the Zou's superconducting Pr-123 samples there should be some Ba atoms at the Pr site; Ba^{2+} on R site dopes additional mobile holes and compensates for the local-

TABLE III. The Rietveld refinement results for fixed N[O(4)]. For notation details see the text.

x	0.00	0.05	0.10	0.15	0.20	0.25	0.30	0.35	0.4	0.5
a(Å)	3.847	3.847	3.855	3.860	3.870	3.868	3.869	3.869	3.868	3.865
b(Å)	3.890	3.889	3.886	3.881	-	-	-	-	-	-
c(Å)	11.696	11.692	11.671	11.660	11.645	11.635	11.608	11.585	11.580	11.563
Gd N	0.847	0.837	0.855	0.917	0.901	0.928	0.988	0.957	0.894	0.890
B(Å)	0.926	0.223	1.250	0.789	2.175	1.735	1.179	0.413	1.562	1.507
Ba N	0.998	0.982	0.976	0.944	0.972	0.905	0.871	0.909	0.808	0.746
B(Å)	3.040	3.488	2.066	0.580	2.336	1.896	1.340	1.765	1.723	1.668
Z	0.1813	0.1810	0.1817	0.1833	0.1815	0.1814	0.1831	0.1801	0.1802	0.1799
Ba_R N	0.00	0.004	0.021	0.040	0.067	0.028	0.002	0.00	0.00	0.00
Pr N	-	0.026	0.050	0.076	0.099	0.124	0.150	0.174	0.199	0.249
B(Å)	-	2.786	2.364	0.878	2.158	1.718	1.162	1.941	1.544	1.490
Cu(2)B(Å)	2.758	2.657	2.374	1.106	2.191	1.995	1.601	0.657	2.009	2.310
Z	0.3508	0.3516	0.3501	0.3514	0.3493	0.349	0.3527	0.3512	0.3507	0.3498
O(1) N	0.815	0.725	0.793	0.881	0.505	0.530	0.530	0.485	0.495	0.480
O(2) Z	0.3872	0.3810	0.3798	0.3732	0.3750	0.3734	0.3744	0.3660	0.3733	0.3758
O(3) Z	0.3680	0.374	0.3753	0.3603	-	-	-	-	-	-
O(4) Z	0.1495	0.1520	0.1437	0.1404	0.1360	0.1376	0.1487	0.1410	0.1515	0.1491
O(5) N	0.175	0.305	0.237	0.209	-	-	-	-	-	-
R_p(%)	10.698	10.426	12.398	11.280	13.353	12.829	12.287	9.436	10.972	12.313
R_{wp}(%)	13.781	13.389	16.128	14.590	17.368	16.653	15.553	12.022	14.165	15.753
R_B(%)	8.11	6.72	7.30	6.68	7.27	6.95	5.85	8.81	6.56	7.30
R_F(%)	7.39	6.75	8.55	7.30	9.53	0.18	7.11	11.17	7.41	9.11
S	1.153	1.135	1.110	1.115	1.128	1.122	1.120	0.751	1.133	1.142

ization of holes by the Pr-O(2,3) hybridization. They mentioned that the substitution of Ba for Pr could be a natural explanation not only for the superconductivity in Pr-123, but also for the elongation of the distances between the CuO_2 planes observed in Ref. 10. It is worthy to note that Zou and Nishihara[12] have also confirmed that, based on the effective magnetic moment of Pr in Pr-123, Ba_R could be a possible interpretation for the superconductivity in Pr-123. Therefore, if in the unit cells with Ba_R superconductivity occurs, the resistivity will decrease at T_m. However, due to the large insulating parts of the sample, which are Pr substituted, the resistivity does not decrease to zero till the Josephson coupling energy between superconducting parts exceeds the thermal energy of the order of k_BT. Then, the superconducting transition occurs. More evidence in support of our claim is that the temperature at which Ba_R occurs in our samples, T_m, has the same value as the superconducting transition temperature of Pr-123 in Ref. 10. Where the Ba_R missubstitution is considerable, the c-x curve in Fig. 11 shows that the changes of c lattice parameter for $0.1 \leqslant x \leqslant 0.25$ has a slightly different x dependence (shown by the dashed line). The Ba_R effect could be the origin of different c-x dependence in the particular range of doping.

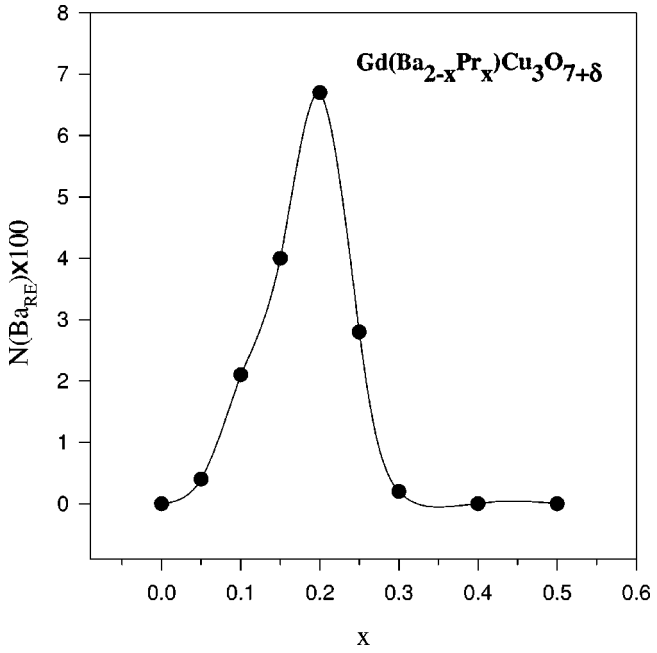

FIG. 10. Site occupation factor percent of Ba atoms at R site vs different amounts of Pr doping (x). The line through the points is a guide to the eye.

The superconducting parts of the samples with transition temperature T_m cannot be the Gd-123 regions because the T_c of Gd-123 is about 92 K for the optimum value of oxygen.[53] Also, the oxygen content for the oxygen deficient Gd-123 with $T_c \sim T_m \sim 80$ K is less than 6.85,[53] but all of our samples have oxygen contents of more than 6.96 (Table II). One scenario for explaining the observed hump anomaly could be the existence of oxygen depleted Gd-123 regions and oxygen rich $Gd(Ba_{2-x}Pr_x)Cu_3O_{7+\delta}$ regions (due to the Pr^{3+} at the Ba^{2+} site). The oxygen depleted Gd-123 regions have T_c

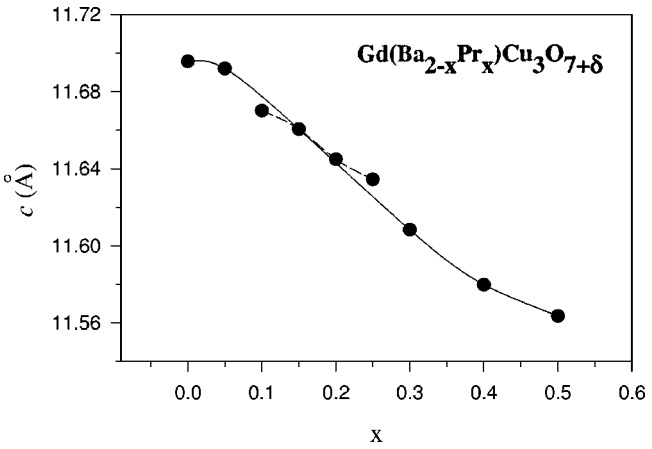

FIG. 11. Variation of the c lattice parameter vs different amounts of Pr doping (x). The dashed line in $0.10 \leqslant x \leqslant 0.25$ shows a different x dependence of c. The lines through the points are guides to the eye.

varying from 90 to 0 K for different oxygen contents. But, the humps occur at almost constant 80 K temperature in all the corresponding samples. Therefore, this possibility should also be ruled out.

The variation of transition temperature T_c vs Pr doping value x is presented in Fig. 7. None of the following earlier proposed models fits to our $T_c(x)$ curve: The linear dependence of T_c for small x, according to the Abrikosov-Gor'kov (AG) model,[54] the combination of the linear and square dependence of x for the AG pair breaking and hole filling models,[55] the general features of the superconducting properties of the matrix-impurity systems, accounted for by a model in which the localized d and f states are nonmagnetic in the sense of the Friedel-Anderson model[56,57] and developed by Kaiser.[58] This formulation, with a more complex x dependence of T_c to account for the variation of the superconducting transition temperature vs the doping, does not fit our data either. Moreover, we could not also find any special x (x_s) for different $T_c(x)$ models for $x<x_s$ and $x>x_s$. It seems that the probable correlation of T_m, due to Ba_R, and T_c, makes it difficult to derive a proper $T_c(x)$ dependence.

Ba_R has also been observed in other HTSCs, which is evidence in support of our proposal. Yang *et al.* found that the resistivity of the Ba-rich Pr-123 ($Pr_{1-x}Ba_{2+x}Cu_3O_7$) samples becomes smaller with the increase of x, together with the elongation of the c axis.[59] Their O K-edge x-ray absorption measurements indicated an increase in the carrier concentration with Ba doping. Merz *et al.*'s EXAFS measurements on the $Pr_{1-x}Ba_{2+x}Cu_3O_7$ samples revealed that upon an increase of x a shift of the Pr $4f-$O $2p_\pi$ band to below the Fermi level is indicated, concurrent with a transfer of doped holes back to the Zhang-Rice singlets.[60] They thus concluded that more Ba-rich samples than the samples they investigated may cause superconductivity in Pr-123 samples. They also mentioned that their observation is consistent with the interpretation of the NMR signal of a Ba-rich $Pr_{1-x}Ba_{2+x}Cu_3O_7$ single crystal given by Pieper and Wolf.[61] Ba^{2+} at the R site could also revive the superconductivity in

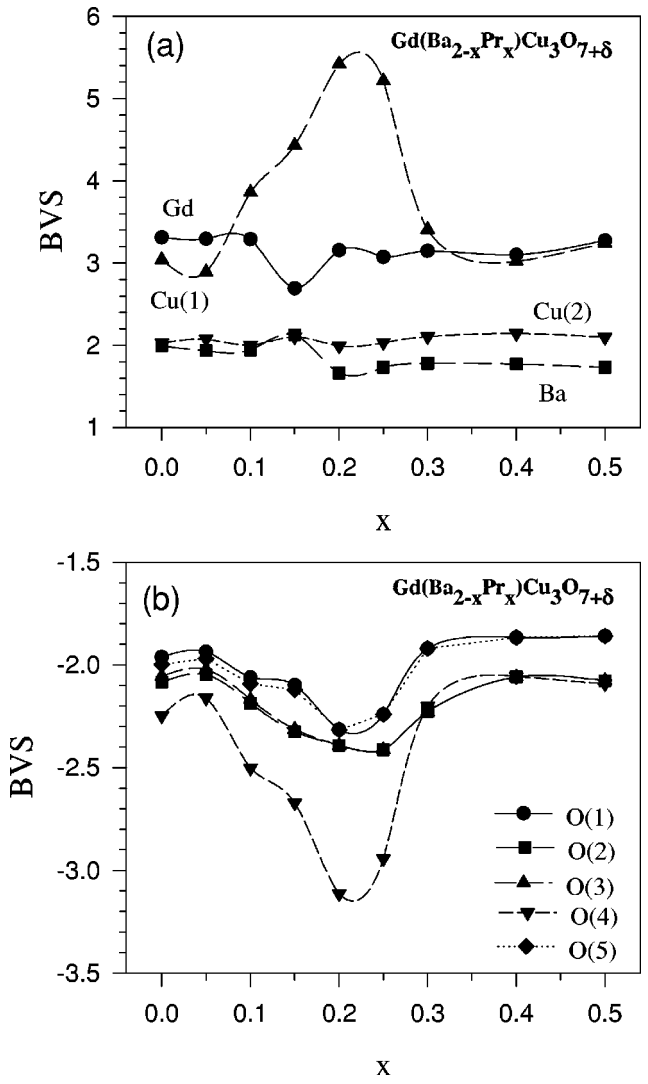

FIG. 12. The BVS of atoms in the $Gd(Ba_{2-x}Pr_x)Cu_3O_{7+\delta}$ compound vs amounts of Pr doping (x) with a fixed occupation factor for O(4). (a) For Cu(1), Cu(2), Gd, and Ba atoms. (b) For O(1), O(2), O(3), O(4), and O(5) atoms. The lines are guides to the eye.

Pr-123, as observed for Ca^{2+}: Thin films of $Pr_{0.5}Ca_{0.5}Ba_2Cu_3O_{7-\delta}$ are superconductors with $T_c \approx 43$ K,[62] and its bulk samples prepared under high pressure are superconductors with $T_c \approx 97$ K.[63] So, there is much evidence for the superconductivity of 123 structures with Ba_R. This effect could also lead to superconductivity and also to a hump on the $\rho(T)$ curve of our samples.

To assure the correctness of the Rietveld refinement results presented in Table III, we have calculated the valences of constituent atoms by the BVS technique, and they are presented in Fig. 12. As is evident, all the valences are reliable within the XRD refinement accuracy except for the O(4) and Cu(1) valences in the range $0.1 \leqslant x \leqslant 0.25$. So, the position of O(4) in this domain should be optimized. The only remaining parameter, which could change to give reliable valences for O(4) and Cu(1), is the site occupation factor of O(4). The importance of the apical oxygen was previously

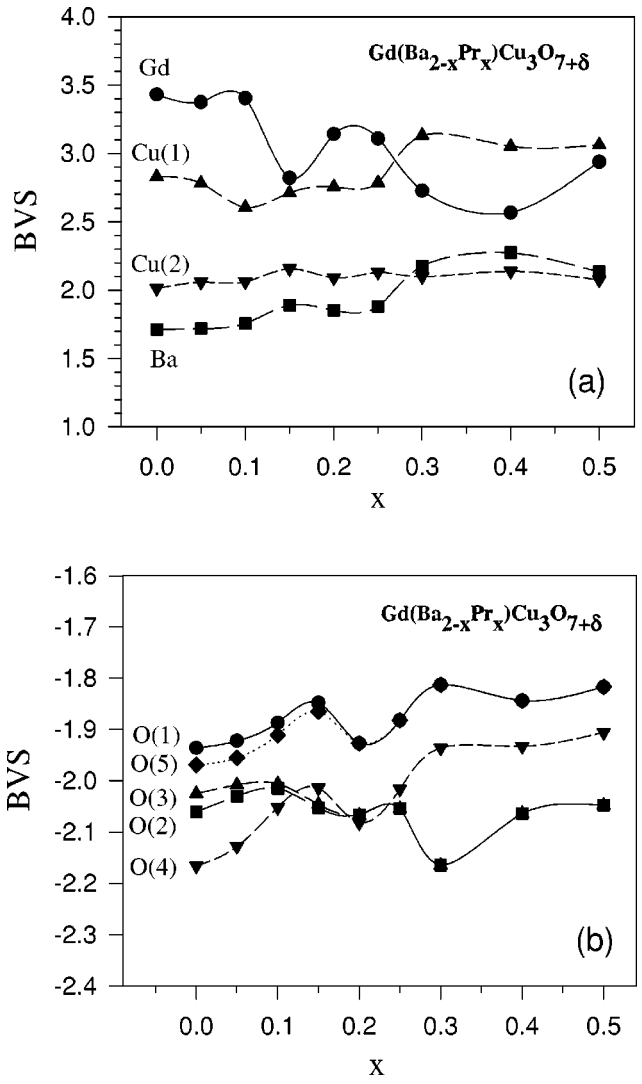

FIG. 13. The BVS of atoms in the $Gd(Ba_{2-x}Pr_x)Cu_3O_{7+\delta}$ compound vs different amounts of Pr doping (x) with a variable occupation factor for O(4). (a) For Cu(1), Cu(2), Gd, and Ba atoms. (b) For O(1), O(2), O(3), O(4), and O(5) atoms. The lines are guides to the eye.

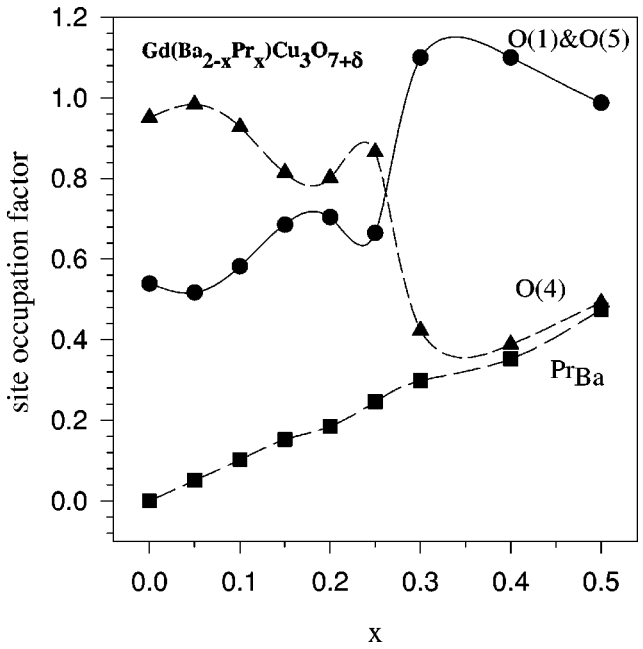

FIG. 14. The site occupation factors for N[O(4)], N[O(1)]=N[O(5)], and $N(Pr_{Ba})$. The lines are guides to the eye.

discussed in the charge transfer (model) between the CuO_2 plane and the Cu-O chain.[64,65] After repeating the refinement with the variable site occupation factor for O(4) in the $0.0 \leqslant x \leqslant 0.50$ range, it was seen that for $0.10 \leqslant x \leqslant 0.30$, the refinement converges to irrelevant values for N and atomic positions. In this domain of x, the expected fixed $Z_{O(4)} = 0.1570$ (Ref. 9) has been used in the refinement. So, the mentioned divergence was solved, and the calculated valences are presented in Fig. 13. The site occupation factor of O(4), Pr, O(1), and O(5) for this case are presented in Fig. 14. It is to be noted that the site occupation factor for Pr is due to replacing Ba at two locations in the unit cell. Therefore, the corresponding number in Table IV is multiplied by 2, as is shown in Fig. 14. Also, the site occupation factors for O(1) and O(5) have been set equal in the refinement, which is also presented in Fig. 14. Now, it is evident that the O(4) and Cu(1) valences have become more reliable; with increasing Pr substitution at the Ba site, the N[O(4)] decreases. The incomplete oxygen content in the O(4) site has also been observed in the quenched $YBa_2Cu_3O_{7-\delta}$ (YBCO) samples.[66]

The final refinement results employing BVS with variable N[O(4)] are presented in Table IV, which, in comparison with Table III, could be considered as final and more reliable data for the corresponding samples. The decrease of the $Z_{O(2)}$ and $Z_{O(3)}$ could be the result of the migration of an O(4) atom from its original site and also to the appearance of Pr^{3+} at the Ba^{2+} site. More evidence for the vacancies appearing at O(4) sites could be the saturation of the total oxygen of the samples of about 7 with increasing x (Table II), while in the $Pr_{1+x}Ba_{2-x}Cu_3O_{7+\delta}$ compound with $0.0 \leqslant x \leqslant 1.0$ the oxygen content increases to 7.31.[34] In other words, for the $Gd(Ba_{1.5}Pr_{0.5})Cu_3O_{7+\delta}$ sample, the 6.96 amount of oxygen is less than the expected value to compensate for the larger charge of Pr^{3+} with respect to the Ba^{2+} charge. With the increase of x, the O(5) occupation increases and the O(1)-O(5) plane becomes more like the CuO_2 plane, while the O(4) migrates from its original site. Hence, the total amount of oxygen in the samples does not exceed 7.09.

Although a more exact and reliable site occupation factor for oxygen atoms should be determined by neutron diffraction refinement, with the help of the BVS technique, the XRD refinement results have become more reliable. On the other hand, the very close neutron scattering length of Ba (0.507×10^{-12} cm), and Pr (0.458×10^{-12} cm) (Ref. 67) prevents one from distinguishing their real positions in the structure. However, due to the small atomic scattering of the oxygen atoms with respect to the other heavy elements in the $Gd(Ba_{2-x}Pr_x)Cu_3O_{7+\delta}$ compound, the determination of oxygen characters is poor.[68] So, a determination of the Pr

TABLE IV. The Rietveld refinement results with variable N[O(4)] and N[O(1)]=N[O(5)]. For notation details see the text.

x	0.00	0.05	0.10	0.15	0.20	0.25	0.30	0.40	0.50
a(Å)	3.847	3.847	3.855	3.860	3.870	3.868	3.869	3.868	3.865
b(Å)	3.890	3.889	3.888	3.881	-	-	-	-	-
c(Å)	11.696	11.692	11.667	11.660	11.645	11.663	11.607	11.579	11.564
Gd N	0.851	0.837	0.858	0.891	0.903	0.903	1.004	0.906	0.898
B(Å)	1.151	0.403	1.214	0.590	1.195	1.039	0.714	0.027	0.226
Ba N	0.999	0.982	0.977	0.937	0.973	0.901	0.811	0.805	0.746
B(Å)	3.241	3.668	2.030	0.380	1.356	1.201	0.875	0.188	0.387
Z	0.1811	0.1808	0.1813	0.1830	0.1813	0.1819	0.1843	0.1817	0.1809
Ba_R N	-	-	-	0.038	0.045	0.025	0.004	0.030	0.019
Pr N	-	0.026	0.051	0.076	0.093	0.123	0.149	0.176	0.237
B(Å)	-	2.966	2.328	0.678	1.177	1.022	0.1818	0.010	0.209
Cu(2)B(Å)	2.954	2.858	2.292	0.970	1.243	1.373	1.341	0.642	1.116
Z	0.3508	0.3515	0.3509	0.3517	0.3504	0.3503	0.3533	0.3501	0.3493
O(1) N	0.539	0.517	0.582	0.685	0.704	0.665	1.0	1.0	0.988
O(2) Z	0.3886	0.3815	0.379	0.367	0.375	0.374	0.367	0.363	0.3701
O(3) Z	0.3707	0.3765	0.380	0.371	-	-	-	-	-
O(4) Z	0.1524	0.1531	0.1570	0.157	0.1570	0.1570	0.1570	0.1596	0.1581
O(4) N	0.951	0.983	0.928	0.815	0.801	0.865	0.423	0.389	0.4923
R_p(%)	10.732	10.444	12.478	11.333	13.393	12.853	12.299	10.969	12.278
R_{wp}(%)	13.809	13.410	16.163	14.631	17.399	16.679	15.538	14.115	15.709
R_B(%)	8.19	6.82	7.38	6.79	7.47	6.97	5.99	6.06	6.60
R_F(%)	7.55	6.79	8.61	7.39	9.57	8.98	6.77	6.70	8.28
S	1.155	1.137	1.112	1.118	1.130	1.123	1.118	1.130	1.139

real position in each 123 compound is a crucial step towards explaining its influence(s).

With Pr substitution at the Ba site, the perovskite substructures containing Pr become similar to the R containing perovskite substructures. So, Pr_{Ba} makes its environment the same as Pr at the rare earth site (Pr_R) but, due to the solubility limit this process can only be followed to a certain extent. The amount of oxygen in $Eu(Ba_{2+x}Pr_x)Cu_3O_{7-\delta}$ for $0.0 \leqslant x \leqslant 0.7$ is less than 6.964,[15,69] in $Er(Ba_{2-x}La_x)Cu_3O_{7-\delta}$ for $0.0 \leqslant x \leqslant 0.3$ is at most 7,[70] and in $Sm(Ba_{2-x}Pr_x)Cu_3O_{7-\delta}$ for $0.0 \leqslant x \leqslant 0.2$ is from 6.96 to 7.04, respectively.[31] This small amount of oxygen, in spite of the appearance of R^{3+} at the Ba^{2+} site, supports our idea that with increasing x the O(4) atom migrates from its original position. This retains a coordination number close to 8 for Pr atoms at the Ba site, and the total oxygen content of the samples remains less than or about 7. Therefore, as we mentioned earlier, it seems that the formation of the incomplete perovskite sublattices in the 123 structure is the principle behind this mis-substitution. Since Pr_{Ba} makes its environment the same as that of Pr at the rare earth site (Pr_R), Pr at Ba or rare earth sites suppresses the superconductivity by the same mechanism(s).

CONCLUSIONS

We have prepared and studied $Gd(Ba_{2-x}Pr_x)Cu_3O_{7+\delta}$ samples. Different lattice parameters and unit cell volume changes with respect to x in comparison with the $(Gd_{1-x}Pr_x)Ba_2Cu_3O_{7-\delta}$ compound, the extra oxygen in the unit cell ($7+\delta \geqslant 6.96$) with respect to the optimum oxygen content in $(Gd_{1-x}Pr_x)Ba_2Cu_3O_{7-\delta}$ samples ($7-\delta \leqslant 6.95$), and the different x_c^{SIT} for the above systems show that, as expected, a Pr atom substitutes at the Ba site. The appearance of the solubility limit O-T phase transition with increasing x, and the absence of a Gd-based impurity phase, comprise additional evidence for the expected structure of Pr_{Ba} in Gd-123.

Based on the Rietveld refinement and BVS technique, we have found that the Ba atom substitution at the rare earth site could lead to superconductivity in some parts of the grains at $T_m \sim 80-90$ K, which appears as a hump on the $\rho(T)$ curve. It is also concluded that with increasing Pr doping, the O(4) atom migrates from its original site, and the O(5) occupation increases. So, with the substitution of Pr at the Ba site, the basic perovskite substructure would become identical with that of Pr at a rare earth site perovskite, and, hence, Pr at Ba or R sites suppresses the superconductivity by the same mechanism(s).

ACKNOWLEDGMENTS

We wish to thank H. Khosroabadi and V. Daadmehr for the technical assistance and valuable discussions, H. Salamati, P. Kameli, and M. Eshraghi for the susceptibility measurements, and M. Sedaghat. This work was supported in part by the Offices of Vice President for Research and Dean of Graduate Studies at Sharif University of Technology.

*Corresponding author: Fax: +98 21 6012983. Email address: akhavan@sharif.edu

[1] Z. Yamani and M. Akhavan, Phys. Rev. B **56**, 7894 (1997).
[2] L. Soderholm, K. Zhang, D. G. Hinks, M. A. Beno, J. D. Jorgensen, C. U. Segre, and I. K. Schuller, Nature (London) **328**, 604 (1987).
[3] J. J. Neumeier, T. Bjornholm, M. B. Maple, and I. K. Schuller, Phys. Rev. Lett. **63**, 2516 (1989).
[4] G. Y. Guo and W. M. Temmerman, Phys. Rev. B **41**, 6372 (1990).
[5] R. Fehrenbacher and T. M. Rice, Phys. Rev. Lett. **70**, 3471 (1993).
[6] H. A. Blackstead and J. D. Dow, Solid State Commun. **115**, 137 (2000), and references therein.
[7] M. Akhavan, Physica B **321**, 265 (2002).
[8] H. A. Blackstead, D. B. Chrisey, J. D. Dow, J. S. Horwitz, A. E. Klunzinger, and D. B. Pulling, Phys. Lett. A **207**, 109 (1995).
[9] M. J. Kramer, K. W. Dennis, D. Falzgraf, R. W. McCallum, S. K. Malik, and W. B. Yelon, Phys. Rev. B **56**, 5512 (1997).
[10] Z. Zou, J. Ye, K. Oka, and Y. Nishihara, Phys. Rev. Lett. **80**, 1074 (1998).
[11] V. N. Narozhnyi and S.-L. Drechsler, Phys. Rev. Lett. **82**, 461 (1999).
[12] Z. Zou and Y. Nishihara, Phys. Rev. Lett. **82**, 462 (1999).
[13] N. Watanabe, K. Kuroda, K. Abe, N. Koshizuka, M. Tagami, and Y. Shiohara, Physica C **300**, 301 (1998).
[14] M. Muroi and R. Street, Physica C **314**, 172 (1999).
[15] Z. Klencsar, E. Kuzmann, Z. Homonnay, A. Vertes, K. Vad, J. Bankuti, T. Racz, M. Bodogh, and I. Kotsis, Physica C **304**, 124 (1998).
[16] H. A. Blackstead and J. D. Dow, Phys. Rev. B **51**, 11 830 (1995).
[17] V. G. Harris, D. J. Fatemi, V. M. Browning, M. S. Osofsky, and T. A. Vanderah, J. Appl. Phys. **83**, 6783 (1998).
[18] M. R. Mohammadizadeh, H. Khosroabadi, and M. Akhavan, Physica B **321**, 301 (2002).
[19] Z. Yamani and M. Akhavan, Supercond. Sci. Technol. **10**, 427 (1997).
[20] D. B. Wiles and R. A. Young, J. Appl. Crystallogr. **14**, 149 (1981); R. A. Young, in *The Rietveld Method*, edited by R. A. Young (Oxford University Press, New York, 1993), p. 1.
[21] Ch. Bertrand, Ph. Galez, R. E. Gladyshevskii, and J. L. Jorda, Physica C **321**, 151 (1999).
[22] I. D. Brown and D. Altermatt, Acta Crystallogr., Sect. B: Struct. Sci. **41**, 244 (1985).
[23] I. D. Brown, J. Solid State Chem. **82**, 122 (1989).
[24] J. L. Tallon, Physica C **168**, 85 (1990).
[25] P. Lundqvist, C. Tengroth, O. Rapp, R. Tellgren, and Z. Hegedus, Physica C **269**, 231 (1996).
[26] M. Izumi, T. Yabe, T. Wada, A. Maeda, K. Uchinokura, S. Tanaka, and H. Asano, Phys. Rev. B **40**, 6771 (1989).
[27] M. Luszczek, W. Sadowski, T. Klimczuk, J. Olchowik, B. Susla, and R. Czajka, Physica C **322**, 57 (1999).
[28] W. H. Tang and J. Gao, Physica C **298**, 66 (1998).
[29] S. Li, E. A. Hayri, K. V. Ramanujachary, and M. Greenblatt, Phys. Rev. B **38**, 2450 (1988).
[30] H. M. Luo, S. Y. Ding, G. X. Lu, B. N. Lin, H. C. Ku, C. H. Lin, H.-C. I. Kao, and J. C. Ho, Supercond. Sci. Technol. **14**, 320 (2001).
[31] L. Colonescu, F. Cairon, J. Berthon, I. Zelenay, and R. Suryanarayanan, Physica B **259–261**, 528 (1999).
[32] G. Cao, Y. Qian, X. Li, Z. Chen, C. Wang, K. Ruan, Y. Qiu, L. Cao, Y. Ge, and Y. Zhang, J. Phys.: Condens. Matter **7**, L287 (1995).
[33] Y. Xu, M. J. Kramer, K. W. Dennis, H. Wu, A. O'Connor, R. W. McCallum, S. K. Malik, and W. B. Yelon, Physica C **333**, 195 (2000).
[34] H. M. Luo, B. N. Lin, Y. H. Lin, H. C. Chiang, Y. Y. Hsu, T. I. Hsu, T. J. Lee, H. C. Ku, C. H. Lin, H.-C. I. Kao, J. B. Shi, J. C. Ho, C. H. Chang, S. R. Hwang, and W.-H. Li, Phys. Rev. B **61**, 14 825 (2000).
[35] M. R. Mohammadizadeh and M. Akhavan, Eur. Phys. J. B **33**, 381 (2003).
[36] Z. Yamani and M. Akhavan, Physica C **268**, 78 (1996); Z. Yamani and M. Akhavan, Supercond. Sci. Technol. **10**, 427 (1997).
[37] J. D. Jorgensen, B. W. Veal, A. P. Paulikas, L. J. Nowicki, G. W. Crabtree, H. Claus, and W. K. Kwok, Phys. Rev. B **41**, 1863 (1990).
[38] M. Covington and L. H. Greene, Phys. Rev. B **62**, 12 440 (2000).
[39] T. Ito, K. Takenaka, and S. Uchida, Phys. Rev. Lett. **70**, 3995 (1993); G. Zolfagharkhani, V. Daadmehr, M. Farzaneh, A. Sedighiani, and M. Akhavan, in *Proceedings of the 1st Regional Conference on Magnetic and Superconducting Materials (MSM-99)*, edited by M. Akhavan, J. Jensen, and K. Kitazawa (World Scientific, Singapore, 2000), Vol. A, p. 175.
[40] A. Carrington, A. P. Mackenzie, C. T. Lin, and J. R. Cooper, Phys. Rev. Lett. **69**, 2855 (1992); B. Moeckly and K. Char, Physica C **265**, 283 (1996).
[41] J. L. Peng, P. Klavins, R. N. Shelton, H. B. Radousky, P. A. Hahn, and L. Bernardez, Phys. Rev. B **40**, 4517 (1989).
[42] K. Kinoshita, A. Matsuda, T. Ishii, N. Suzuki, H. Shibata, T. Watanabe, and T. Yamada, J. Appl. Phys. **27**, L795 (1988).
[43] M. Kakihana, S. Kato, V. Petrykin, J. Backstrom, L. Borjesson, and M. Osada, Physica C **321**, 74 (1999).
[44] A. P. Litvinchuk, L. Brjesson, C. Thomsen, and P. Berastegui, J. Phys. Chem. Solids **59**, 2000 (1998).
[45] S. Horii, U. Mizutani, H. Ikuta, Y. Yamada, J. H. Ye, A. Matsushita, N. E. Hussey, H. Takagi, and I. Hirabayashi, Phys. Rev. B **61**, 6327 (2000).
[46] R. S. Gonnelli, V. A. Stepanov, A. Morello, G. A. Ummarino, D. Daghero, F. Licci, and G. Ubertalli, Physica C **341–348**, 1779 (2000).
[47] E. Maiser, P. Fournier, J.-L. Peng, F. M. Araujo-Moreira, T. Venkatesan, R. L. Greene, and G. Czjzek, Physica C **297**, 15 (1998).
[48] H. Khosroabadi, V. Daadmehr, and M. Akhavan, Mod. Phys. Lett. B **16**, 943 (2002).
[49] M. R. Mohammadizadeh and M. Akhavan, Supercond. Sci. Technol. **16**, 538 (2003); Physica C **390**, 134 (2003); H. Shakeripour and M. Akhavan, Supercond. Sci. Technol. **14**, 234 (2001).
[50] X. Zhou, J. Li, F. Wu, C. Dong, J. Li, S. Jia, Y. Yao, and Z. Zhao, Supercond. Sci. Technol. **7**, 832 (1994).
[51] A. Gerber, T. Grenet, M. Cyrot, and J. Beille, Phys. Rev. Lett. **65**, 3201 (1990).
[52] V. N. Narozhnyi, D. Eckert, K. A. Nenkov, G. Fuchs, K.-H. Muller, and T. G. Uvarova, cond-mat/9909107 (unpublished).
[53] K. Koyama, T. Tange, T. Saito, and K. Mizuno, Physica B **281&282**, 909 (2000).
[54] A. A. Abrikosov and L. P. Gor'kov, Zh. Eksp. Teor. Fiz. **39**, 1781 (1960) [Sov. Phys. JETP **12**, 1243 (1961)].
[55] W. H. Tang and J. Gao, Physica C **315**, 59 (1999).

[56] J. Friedel, Nuovo Cimento Suppl. **12**, 1861 (1958).
[57] P. W. Anderson, Phys. Rev. **124**, 41 (1961).
[58] A. B. Kaiser, J. Phys. C **3**, 409 (1970).
[59] H. D. Yang, I. P. Hong, S. Chatterjee, P. Nachimuthu, J. M. Chen, and J.-Y. Lin, Physica C **341–348**, 411 (2000).
[60] M. Merz, S. Gerhold, N. Nucker, C. A. Kuntscher, B. Burbulla, P. Schweiss, S. Schuppler, V. Chakarian, J. Freeland, Y. U. Idzerda, M. Klaser, G. Muller-Vogt, and Th. Wolf, Phys. Rev. B **60**, 9317 (1999).
[61] M. W. Pieper and Th. Wolf (unpublished).
[62] D. P. Norton, D. H. Lowndes, B. C. Sales, J. D. Budai, B. C. Chakoumakos, and H. R. Kerchner, Phys. Rev. Lett. **66**, 1537 (1991).
[63] Y. S. Yao, Y. F. Xiong, D. Jin, J. W. Li, F. Wu, J. L. Luo, and Z. X. Zhao, Physica C **282–287**, 49 (1997).
[64] M. R. Mohammadizadeh and M. Akhavan (unpublished).
[65] J. D. Jorgensen, Phys. Today **44**(6), 34 (1991).
[66] J. D. Jorgensen, B. W. Veal, W. K. Kwok, G. W. Crabtree, A. Umezawa, L. J. Nowicki, and A. P. Paulikas, Phys. Rev. B **36**, 5731 (1987).
[67] V. F. Sears, Neutron News **3**, 26 (1992).
[68] F. Izumi, H. Asano, T. Ishigaki, E. Takayama-Muromachi, Y. Uchida, N. Watanabe, and T. Nishikawa, Jpn. J. Appl. Phys. **26**, L649 (1987).
[69] Z. Klencsar, E. Kuzmann, A. Vertes, P. C. M. Gubbens, A. M. Kraan, M. Bodogh, and I. Kotsis, Physica C **329**, 1 (2000).
[70] D. Wagener, M. Buchgeister, W. Hiller, S. M. Hosseini, and K. Kopitzki, Supercond. Sci. Technol. **4**, S211 (1991).